

# BEAM DYNAMICS CALCULATIONS FOR THE SPring-8 PHOTOINJECTOR SYSTEM USING MULTIPLE BEAM ENVELOPE EQUATIONS

A. Mizuno\*, H. Dewa, T. Taniuchi, H. Tomizawa and H. Hanaki  
 JASRI/SPring-8, 1-1-1, Koto, Sayo, Hyogo, 679-5198, Japan  
 E. Hotta, Department of Energy Sciences, Tokyo Institute of Technology,  
 Nagatsuta-cho, Midori-ku, Yokohama, Kanagawa, 226-8502, Japan

## Abstract

A new semi-analytical method of investigating the beam dynamics for electron injectors was developed. In this method, a short bunched electron beam is assumed to be an ensemble of several segmentation pieces in both the longitudinal and the transverse directions. The trajectory of each electron in the segmentation pieces is solved by the beam envelope equations. The shape of the entire bunch is consequently calculated, and thus the emittances can be obtained from weighted mean values of the solutions for the obtained electron trajectories. Using this method, the beam dynamics calculation for the SPring-8 photoinjector system was performed while taking into account the space charge fields, the image charge fields at a cathode surface, the electromagnetic fields of the rf gun cavity and the following accelerator structure, and the fields of solenoidal coils. In this paper, we discuss applicable conditions for this method by comparing calculation results of this method and those of a particle-tracking simulation code.

## INTRODUCTION

The emittance calculation technique is important in the design of electron injectors for x-ray free electron lasers. There have been many analytical solutions for beam dynamics though it is difficult to accurately calculate practical bunch shapes and detailed emittance behavior. Meanwhile, particle-tracking simulation codes are useful to calculate dynamics of practical beams. However, the calculated emittances often depend on the number of particles.

To overcome the above problems and for accurate calculations of short bunched electron beam dynamics, the authors developed a new semi-analytical solution by combining an analytical method and a simulation method [1] using the multiple beam envelope equations.

In this method, a short bunched electron beam is assumed to be an ensemble of several segmentation pieces in both the longitudinal and the transverse directions. The trajectory of each electron in the segmentation pieces is solved by the beam envelope equations. The shape of the entire bunch is consequently calculated, and thus the accurate emittances were successfully calculated from weighted mean values of the solutions for the each obtained electron trajectory.

\* mizuno@spring8.or.jp

In Ref [1], the authors discussed the semi-analytical solution method of beam dynamics mainly about space charge effects. Therefore, only the beam dynamics in an rf gun cavity and free space including image charge effects for a cathode were described. However, to analyze the beam dynamics of practical electron injectors, it is necessary to calculate beam traces with solenoidal coil focusing effects and in accelerator structures.

In this paper, we describe methods for calculating beam traces in solenoidal fields and in accelerator structures using the semi-analytical method described in Ref [1]. We also show the beam dynamics calculation results for the SPring-8 photoinjector system and compare them with results of a particle-tracking simulation code.

## OUTLINE OF MULTIPLE BEAM ENVELOPE EQUATIONS

The initial bunch model used for the semi-analytical method in Ref [1] is shown in Fig. 1. The bunch is longitudinally divided into  $m$  slices and transversely  $n$  parts. The each electron is located at each segmentation boundary and traced by the beam envelope equation.

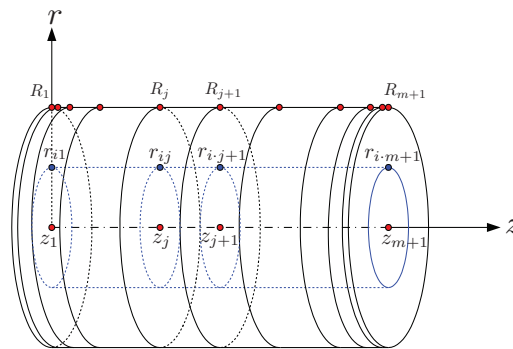


Figure 1: The initial bunch segmentation model for the multiple beam envelope equations.

For the longitudinal envelope equations, the electrons  $z_j$  ( $j = 1, \dots, m + 1$ ) are set on the beam axis. For the transverse equations, the electrons  $r_{ij}$  ( $i = 1, \dots, n$  and  $j = 1, \dots, m + 1$ ) which represent the parts inside the bunch are set at each transverse segmentation boundary,  $R_j$  are set at circumference of the bunch.  $\beta_j$  are also defined as the normalized longitudinal velocity of each elec-

tron having suffix  $j$  for differential equations in terms of electron energy. Note that energy of electrons at  $z_j$ ,  $r_{ij}$  ( $i = 1, \dots, n$ ) and  $R_j$  are the same. These differential equations make up a set of two dimensional multiple beam envelope equations containing  $(n+3)(m+1)$  dependent variables which are described in Ref [1] as follows:

$$\frac{d^2 R_j}{dt^2} = -\frac{e}{\gamma_j m_0} \left( \frac{E_{r.sc}}{\gamma_j^2} - E_r + \beta_j c B_\theta + \frac{\beta_j}{c} \cdot \frac{dR_j}{dt} E_z \right) \quad (1)$$

$$\frac{d^2 r_{ij}}{dt^2} = -\frac{e}{\gamma_j m_0} \left( \frac{E_{r.sc}}{\gamma_j^2} - E_r + \beta_j c B_\theta + \frac{\beta_j}{c} \cdot \frac{dr_{ij}}{dt} E_z \right) \quad (2)$$

$$\frac{d^2 z_j}{dt^2} = -\frac{e}{\gamma_j^3 m_0} (E_{\xi.sc} + E_z) \quad (3)$$

$$\frac{d\beta_j}{dt} = \frac{1}{c} \frac{dz_j}{dt^2} \quad (4)$$

where  $E_{r.sc}$  and  $E_{\xi.sc}$  are summations of transverse and longitudinal space charge fields from each longitudinal slice,  $E_r$ ,  $B_\theta$  and  $E_z$  are external electric and magnetic fields.

### Calculations with solenoidal focusing effects

To calculate solenoidal field focusing effects, one candidate method is that focusing terms  $\left(\frac{eB_z}{2m_0\gamma_j}\right)^2 R_j$  and  $\left(\frac{eB_z}{2m_0\gamma_j}\right)^2 r_{ij}$  should be added in Eq. 1 and 2 respectively. Though when the electrons are over-focused,  $R_j$  or  $r_{ij}$  become negative values and the differential equations can not be calculated at this point. Therefore, we decide to add the differential equations for theta direction to the multiple beam envelope equations. The equation for theta direction can be derived from Eq.2 in Ref [1]:

$$\frac{d^2 \Theta}{dt^2} = -\frac{e}{\gamma_j m_0 A} \left( \beta_j c B_r - \frac{dA}{dt} B_z + \frac{A\beta_j}{c} E_z \frac{d\Theta}{dt} \right) - \frac{2}{A} \frac{dA}{dt} \frac{d\Theta}{dt} \quad (5)$$

where  $A$  represents  $R_j$  or  $r_{ij}$ ,  $\Theta$  represents  $\theta$  of each electron,  $B_r$  and  $B_z$  are solenoidal fields.

For the transverse equations, the following terms have to be added to the right-hand side of Eq. 1 and 2:

$$-\frac{e}{\gamma_j m_0} \cdot A \frac{d\Theta}{dt} B_z + A \left( \frac{d\Theta}{dt} \right)^2 \quad (6)$$

These envelope equations can be numerically analyzed with a data file set of solenoidal fields.

### Calculations in accelerator structures

Fields of a traveling wave accelerator structure can also be prepared as a data file set and be included in the multiple beam envelope equations, though in practical, fields of

a long accelerator structure are hard for calculation. Therefore, we divide the structure into 3 sections, which are from the coupler cell to the third cell, last 3 cells, and the other normal cell section. For each section, we have prepared two kinds of field mapping data, which are calculated with the Neumann and Dirichlet boundary conditions for both longitudinal ends, to represent the traveling wave fields as follows:

$$\begin{aligned} E_z &= E_n(z) \cos(\omega t) - E_d(z) \sin(\omega t) \\ B_\theta &= B_n(z) \sin(\omega t) + B_d(z) \cos(\omega t). \end{aligned} \quad (7)$$

where  $E_n(z)$  and  $B_n(z)$  are the Neumann condition data,  $E_d(z)$  and  $B_d(z)$  are the Dirichlet condition data. Note that for the normal section, the structure is periodical, therefore only 1.5 cells are necessary to be prepared the field mapping data since the structure is  $2/3 \pi$  mode. Calculated data for these 3 sections are connected smoothly to represent the entire field of an accelerator structure.

## BEAM DYNAMICS CALCULATIONS

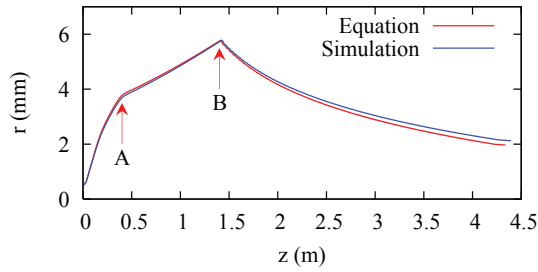
As examples for beam dynamics analysis with solenoidal and accelerator structure fields using the multiple beam envelope equations, calculations for the SPring-8 photoinjector system are discussed here. The system consists of a single cell S-band rf gun cavity with copper cathode [2], two solenoidal coils after the rf gun cavity and a 3-m long traveling wave accelerator structure whose entrance is located at 1.4 m from the cathode surface. The beam energy is 3.7 MeV at the exit of the rf gun cavity and 30.0 MeV at the exit of the accelerator structure.

Figure 2 shows calculation results for the multiple beam envelope equations along with those for the three-dimensional particle-tracking simulation code [3] developed by the authors. The number of particles used in the simulation code is  $2 \times 10^4$ . The manner of bunch segmentation is the same as that shown in Fig. 1, where  $m = 10$ ,  $n = 10$ ,  $z_1 = -6$  mm and  $z_{m+1} = 0$ . The lengths of the segmentation slices at both ends of the bunch are set to be shorter than that of the middle slices as illustrated in Fig. 1. The parameters for the calculations are listed in Table 1, which are typical parameters for the photoinjector system.

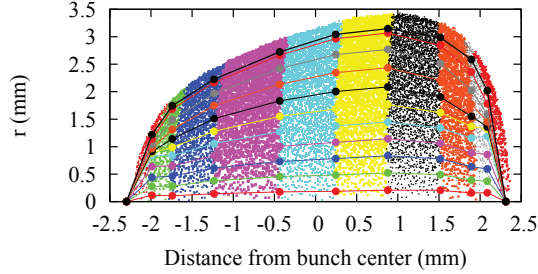
Table 1: Parameters for beam dynamics calculations for the SPring-8 photoinjector system.

Laser length	20 ps uniform
Laser spot size	$\phi$ 1.2 mm uniform
Charge per bunch	0.4 nC
Maximum electric field on the cathode surface	157.0 MV/m
Initial rf phase	sin 5 deg.
Initial emittance	0 mrad

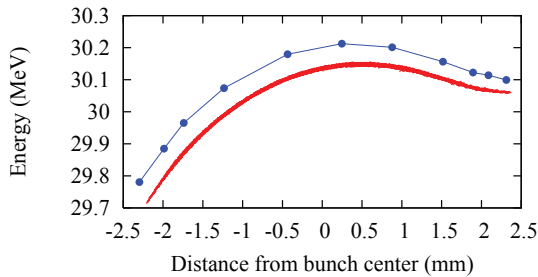
Figure 2(a) shows the calculated time evolutions of the rms transverse beam radius. The cathode surface is located



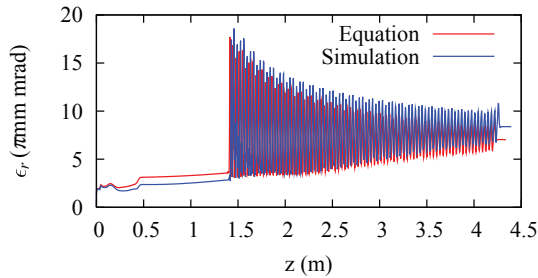
(a) Time evolutions of transverse rms beam radius.



(b) Bunch shapes at the exit of the accelerator structure.



(c) Energy distributions at the exit of the accelerator structure.



(d) Time evolutions of rms r-emittances.

Figure 2: Beam dynamics calculations for the SPring-8 photoinjector system with weak focusing fields. A charge is 0.4 nC per bunch.

at  $z = 0$  m. The beam is focused at point A, which is a position of the solenoidal coils, and also strongly focused at point B which is the entrance of the accelerator structure.

Figure 2(b) shows the bunch shapes at the exit of the accelerator structure. Each dot on the solid lines is an electron traced using the envelope equations. The clouds of small dots are the particles in the simulation. The particles are color coded according to the initial longitudinal segmentation slices used in the multiple envelope equations. In calculation using the multiple envelope equations, each slice must be separated by a plane perpendicular to the  $z$

axis [1] according to the assumption in the bunch segmentation model. In Fig. 2(b), each slice is not warped therefore the calculation is expected to be accurate.

Figure 2(c) shows the energy distributions in the bunch at the exit of the accelerator structure, and Fig. 2(d) shows the time evolutions of normalized r-emittances, which are defined as:

$$\epsilon_r \equiv \langle \gamma \rangle \langle \beta \rangle \sqrt{\langle r^2 \rangle \langle r'^2 \rangle - \langle r \cdot r' \rangle^2}. \quad (8)$$

The r-emittances oscillates in the accelerator structure because the beam is focused at the entrance of each cell and de-focused at the exit. The results of the envelope equations and those of the simulation show good agreement.

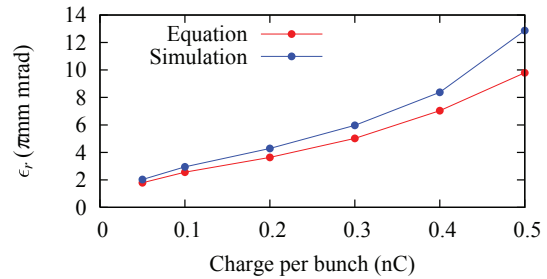


Figure 3: Emittance dependence on charge per bunch.

Figure 3 shows the emittance dependence on charge per bunch at the exit of the accelerator structure. When the charge goes up to 0.5 nC per bunch, the beam envelope is touched the aperture of the entrance of the accelerator structure at point B shown in Fig. 2(a). Therefore, we plot the emittances less than 0.5 nC per bunch. Emittance dependence on charge per bunch obtained by the envelope equations is agree with that by the simulation. Though the emittances by the envelope equations are lower than those by the simulation.

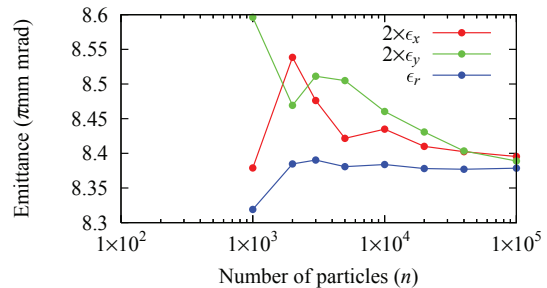
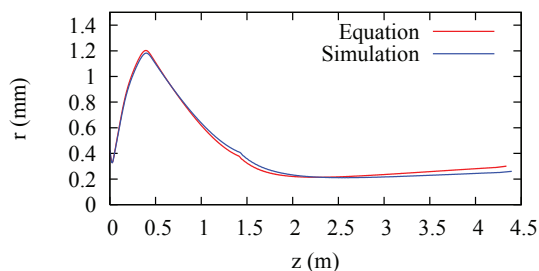


Figure 4: Emittance dependence on number of particles in the simulation. A charge is 0.4 nC per bunch.

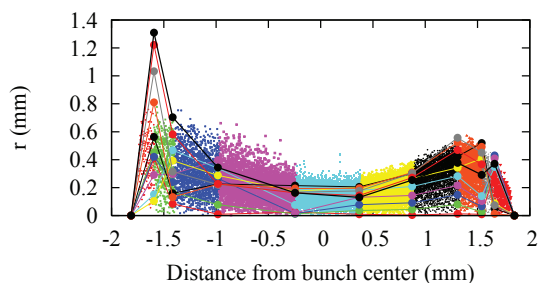
Figure 4 shows the emittance dependence on the number of particles in the simulation when the charge is 0.4 nC per bunch.  $\epsilon_x$ ,  $\epsilon_y$  and  $\epsilon_r$  are plotted since the simulation code is three-dimensional. These emittances are different each other with the small number of particles. Though they tend to be reduced with increasing the number of particles, and

are expected to be converged to the same values. Therefore, the emittance is expected to become closer to that calculated by the envelope equations when the number of particles becomes infinity.

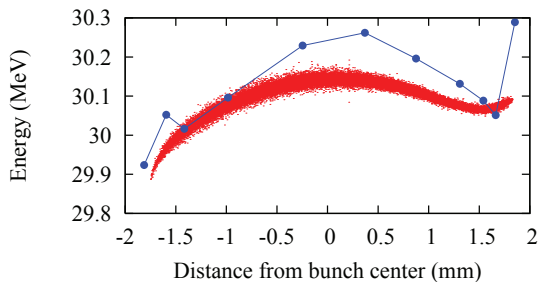
Calculation time of the envelope equations is much shorter than that of the simulation. Whereas it is 9400 hours for the simulation when  $n = 1 \times 10^5$ , it is 7 hours for the envelope equations using Octave with a single core of Xeon W5590 3.33 GHz.



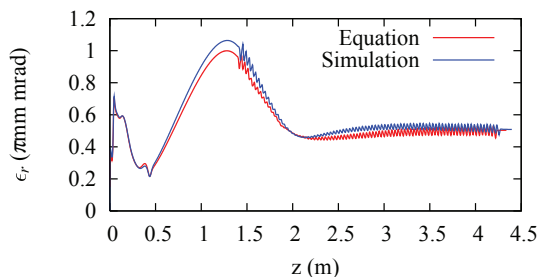
(a) Time evolutions of transverse rms beam radius.



(b) Bunch shapes at the exit of the accelerator structure.



(c) Energy distributions at the exit of the accelerator structure.



(d) Time evolutions of rms r-emittances.

Figure 5: Beam dynamics calculations for the SPring-8 photoinjector system with strong focusing fields. A charge is 50 pC per bunch.

In Fig. 2, the solenoidal field is set to be weaker not to make a waist point in the trace. In contrast beam dynamics

calculation results with stronger solenoidal fields are shown in Fig. 5. The transverse beam radius is shown in Fig. 5(a). The beam is strongly focused at position of the solenoidal coils and a waist point appears at around  $z = 2$  m, which is in the accelerator structure.

The over-focused bunch shapes at the exit of the accelerator structure and the time evolutions of emittance are shown in Fig. 5(b) and 5(d). The emittance and the bunch shape calculated by the envelope equations coincides with those by the simulation. In contrast, each solid line in a calculated bunch shape, which represents particle position inside the bunch and is initially lined in order in the transverse direction, becomes to intercross. The emittance is calculated from weighted mean values of solutions for each electron trajectories [1], therefore the emittance can not be calculated accurately. The energy distributions in the bunch shown in Fig.5(c) is not also calculated correctly.

This is caused by a high charge density at the waist point even if a charge per bunch is 50 pC.

## SUMMARY

We upgraded the multiple beam envelope equations, which were described by the authors in Ref. [1], to analyze beam dynamics in solenoidal fields and in accelerator structures. The envelope equations for theta direction are added to the multiple beam envelope equations for analysis in solenoidal fields.

We have performed the beam dynamics calculations for the SPring-8 photoinjector system by the multiple beam envelope equations and the particle-tracking code. With weaker solenoidal field not to make a waist point in the trace, the bunch shape and the energy distribution in the bunch obtained by the multiple envelope equations agree with those obtained by the simulation, when a charge per bunch is less than 0.4 nC. The emittances obtained by the envelope equations are expected to coincide with converged values obtained by the simulation.

When the beam is over-focused and a waist point appears in the trace, each electron, which is initially lined transversely in order in the bunch, becomes to intercross when a charge per bunch is even 50 pC. Therefore the beam dynamics calculations can not be performed correctly. This is a limitation for the multiple beam envelope equations.

As long as the beam is not over-focused, this semi-analytical method using the multiple beam envelope equations have advantages over methods using particle-tracking simulation codes on accurately calculating emittance and shorter calculation time.

## REFERENCES

- [1] A. Mizuno *et al.*, Phys. Rev. ST Accel. Beams **15**, 064201 (2012).
- [2] T. Taniuchi *et al.*, in *Proceedings of the 21th International Linac Conference, Gyeongju, Korea* (2002), p.683.
- [3] A. Mizuno *et al.*, Nucl. Instrum. Methods Phys. Res., Sect. A **528** 387 (2004).